# SAND REPORT

SAND2004-6434
Unlimited Release
Printed December 2004

# Characterization of a New Class of Surface Micromachined Pumps

Paul C. Galambos

Prepared by
Sandia National Laboratories
Albuquerque, New Mexico  87185 and Livermore, California  94550

Sandia is a multiprogram laboratory operated by Sandia Corporation,
a Lockheed Martin Company, for the United States Department of Energy's
National Nuclear Security Administration under Contract DE-AC04-94-AL85000.



Sandia National Laboratories

Issued by Sandia National Laboratories, operated for the United States Department of Energy by Sandia Corporation.



Available to DOE and DOE contractors from
U.S. Department of Energy
Office of Scientific and Technical Information
P.O. Box 62
Oak Ridge, TN 37831

Telephone: (865)576-8401
Facsimile: (865)576-5728
E-Mail: reports@adonis.osti.gov
Online ordering: http://www.doe.gov/bridge

Available to the public from
U.S. Department of Commerce
National Technical Information Service
5285 Port Royal Rd
Springfield, VA 22161

Telephone: (800)553-6847
Facsimile: (703)605-6900
E-Mail: orders@ntis.fedworld.gov
Online order: http://www.ntis.gov/help/ordermethods.asp?loc=7-4-0#online

SAND2004-6434
Unlimited Release
Printed December 2004

# Characterization of a New Class of Surface Micromachined Pumps

Paul C. Galambos
MEMS Device Technologies

Sandia National Laboratories
P.O. Box 5800
Albuquerque, New Mexico 87185-1080

## Abstract

This is the latest in a series of LDRD's that we have been conducting with Florida State University/Florida A&M University (FSU/FAMU) under the campus executive program. This research builds on the earlier projects; 'Development of Highly Integrated Magnetically and Electrostatically Actuated Micropumps' (SAND2003-4674) and 'Development of Magnetically and Electrostatically Driven Surface Micromachined Pumps' (SAND2002-0704P). In this year's LDRD we designed 2nd generation of surface micromachined (SMM) gear and viscous pumps. Two SUMMiT™ modules full of design variations of these pumps were fabricated and one SwIFT™ module is still in fabrication. The SwIFT™ fabrication process results in a transparent pump housing cover that will enable visualization inside the pumps. Since the SwIFT™ pumps have not been tested as they are still in fabrication, this report will focus on the 2nd generation SUMMiT™ designs. Pump testing (pressure vs. flow) was conducted on several of the SUMMiT™ designs resulting in the first pump curve for this class of SMM pumps. A pump curve was generated for the higher torque 2nd generation gear pump designed by Jason Hendrix of FSU. The pump maximum flow rate at zero head was 6.5 nl/s for a 30V, 30 Hz square wave signal. This level of flow rate would be more than adequate for our typical SMM SUMMiT™ or SwIFT™ channels which have typical volumes on the order of 50 pl.

Acknowledgements:

Pump testing was accomplished at Sandia primarily by two summer students; Jason Hendrix from FSU and Troy Lionberger, now at the University of Michigan. I would like to acknowledge their hard work on this and other projects this past summer. Another summer student Brian Sosnowchick,, now at the University of California at Berkeley, and Jason Hendrix designed the 2nd generation pump/actuator/transmission modules. The pumps were powered by custom designed power amplifiers designed by Ken Pohl (dept 1769). I would also like to thank Dean Chen and Dr Yousef Haik of FSU/FAMU and Dr. Paul Robinson, the campus executive for FSU. Finally I would like to thank the MDL staff and operators for building the pumps and Randy Shul and Sarah Rich for Bosch etching the connecting holes from the back.

**Intentionally Left Blank**

## TABLE OF CONTENTS

## Introduction

This report summarizes the results of this past year's campus executive LDRD with FSU/FAMU (Florida State University/Florida Agricultural and Mechanical University – combined engineering college). This year's work builds on the previous year's LDRD with FSU/FAMU in the area of micropumps – SAND2003-4674 'Development of Highly Integrated Magnetically and Electrostatically Actuated Micropumps' in which the 1$^{st}$ generation surface micromachined (SMM) gear and viscous pumps were tested. The 1$^{st}$ generation pump testing demonstrated that these pumps were capable of moving fluid but were determined to be underpowered. As a result this year higher torque 2$^{nd}$ generation pumps were designed, fabricated and tested and the first pump curve for this class of SMM pumps was generated. All the pumps are electrostatically actuated. While we have designed some magnetically actuatable SMM pumps they have not yet been characterized. Therefore in this report the discussion will be confined to electrostatically actuated micropumps.

The micropump is a key component of microfluidic systems. In particular a fully integrated on-chip microfluidic microsystem, such as would be required for the most sophisticated, smallest volume chemical and/or biological analysis system (μTAS – Micro Total (chemical) Analytical System), requires an integrated micropump for precise small volume solution delivery (picoliter to femtoliter volumes), flow control and constituent separation and concentration [1]. As one minimizes volume requirements and switching times for fluid delivery smaller and more integrated micropumps are required.

Surface micromachining provides a useful platform for the fabrication of such a micropump and the associated integrated micro and/or nano-scale system. Modifications to sophisticated SMM fabrication processes, the SUMMiT$^{TM}$ and SwIFT$^{TM}$ processes (www.mdl.sandia.gov), allow very small dimension (0.1 to 0.01 micron) channels and other structures to be fabricated. Typical SMM channels and structures (1 micron dimension) then act as the packaging that contains and supports the nano-scale system. SMM micropumps can perform the important fluid delivery function for the nano-fluidic components and for integrated on-chip microfluidic systems.

At the SMM scale many researchers have gone away from mechanical pumps because the inertia effects typically utilized to generate fluid motion at the macro-scale are much smaller at the micro-scale and are overpowered by viscous resistance to fluid motion, which is much higher at the large surface to volume ratios and small channel dimensions of SMM microfluidics. The pumping method recommended by many researchers for the SMM scale is electrokinetic (EKP – ElectroKinetic Pumping). In this method charged components of a solution are moved by electric fields and pull the rest of the solution along with them. Impressive pressures have been generated by these pumps (10,000 psi [2]), however efficiencies are generally low (<5% [3]), voltage requirements are high (1000 V [2]) and pump operation and performance are dependent on control over the electrical properties of the pumped liquid (dielectric constant, conductivity, pH).

Non-inertia based mechanical pumps can be categorized as positive displacement, viscous drag or peristaltic pumps and can move fluid at SMM scales while avoiding problems associated with EKP – specifically sensitivity to solution electrical properties. Previous theoretical investigations of SMM viscous drag and gear pumps [4] indicate that they can potentially operate at high efficiency (approaching 30%). In addition, electrostatically actuated micropumps draw very little current and therefore operate at low power levels. Therefore in this LDRD characterization of non-inertial mechanical, electrostatically actuated SMM micropumps in terms of flow rate and pressure generated is undertaken in order to determine if they can indeed supply the need for a fluid insensitive, integrated micropump.

The remainder of this LDRD report will detail: (1) 2$^{nd}$ generation SUMMiT$^{TM}$ pump designs, (2) 2$^{nd}$ generation pump testing, and (3) the pump curve for the 2$^{nd}$ generation gear pump.

# SUMMiT pump designs – 2nd generation

The key finding from the testing of the 1st generation of pumps was that the actuator was too small for the pump. Therefore the redesigned actuator/transmission/pump integrated on-chip SMM assemblies utilized higher torque actuators, and larger gear ratio transmissions (more torque, lower RPM).

Redesigned (higher torque) TRA (Torsional Ratcheting Actuator)

Fortunately the requirement for a higher force torsional actuator coincided with the completion and initial characterization of a higher torque TRA by Jeff Lanz (1769). The results from Jeff's work on an improved TRA can be summarized as [5]:

(1) Increase in the number of gear teeth from 164 to 240. Since force and torque are directly proportional to the number of gear teeth this is theoretically an increase in torque of 240/164 = 1.46 or 64%.
(2) Reduction in gap between teeth from 2 microns to 1.5 microns. Since force and torque are directly proportional to this gap this should result in an increase in torque of 2/1.5 = 1.33 or 33%. The combined effect of items (1) and (2) in this list is a 100% increase in torque or doubling the torque in the new actuator (2nd generation pumps) as compared to the old actuator (1st generation pumps).
(3) Reduction in ratchet stroke length corresponding to increase in teeth. Now 240 ratchet actuations (clicks) are required for a complete revolution of the TRA drive gear.
(4) Better stops to reduce the incidence of skips – actuations that move more than one ratchet tooth.

The redesign was largely successful. Fig. 1 shows a plot of force as a function of voltage for 3 different TRA designs from [5]. The diamonds are for the old TRA while the triangles are for the new redesigned TRA. The redesigned TRA delivers greater than three times the force as the old TRA at the same voltage. Since force is proportional to voltage squared for a comb drive, a curve fit of force vs. voltage squared for the data below yields a constant (the slope of the least squares curve fit) that allows direct comparison of the two designs.

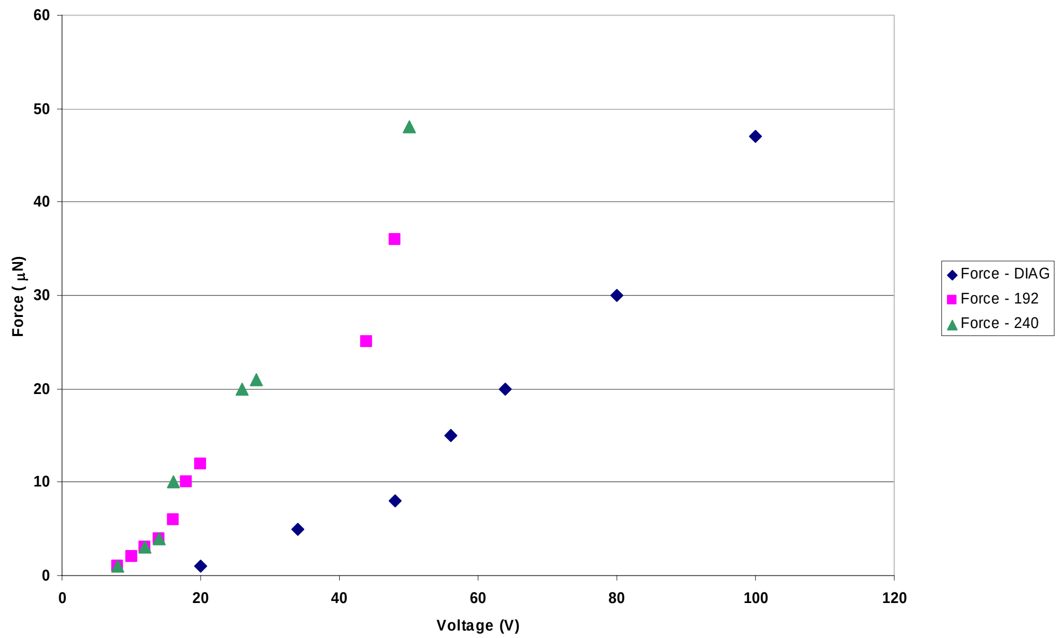


Figure 1. Force as a function of applied voltage for old (diamond) and new (triangle) TRA designs [5].

The results of the curve fits are summarized in Eqn. (1):

$$F = 0.005 \cdot V^2 \quad (old\ TRA) \qquad \text{Eqn (1)}$$

$$F = 0.0185 \cdot V^2 \quad (new\ TRA) \quad \text{Eqn (2)}$$

Where F is the tangential force delivered to the first gear in the transmission by the TRA ring gear in μN and V is the applied voltage. In terms of torque (T - μN-μm) for the 340 μm radius TRA drive gear (both old and new TRA designs) the relationship is:

$$T = 1.73 \cdot V^2 \quad (old\ TRA) \quad \text{Eqn (3)}$$

$$T = 6.29 \cdot V^2 \quad (new\ TRA) \quad \text{Eqn (4)}$$

## Transmissions

There were two different transmission designs used with the old TRA on the 1st generation SMM micropumps (RS275 modules 3 and 4). These designs had transmissions with lower gear ratios for faster (higher pump gear RPM for the same drive signal frequency) and therefore lower torque delivery to the pump than on the 2nd generation designs. The new transmission designs (RS415 module 7 and RS424 module 2) deliver more torque for a given input force from the TRA to the pumping gear. Consider RS415 module 7 designed by Jason Hendrix. There are new viscous spiral, plate and impeller pump designs, and a crescent gear pump design. There are 3 transmissions – one for the gear pump and two different gear ratio designs for the viscous pumps. Fig. 2 shows the new designs from RS415.

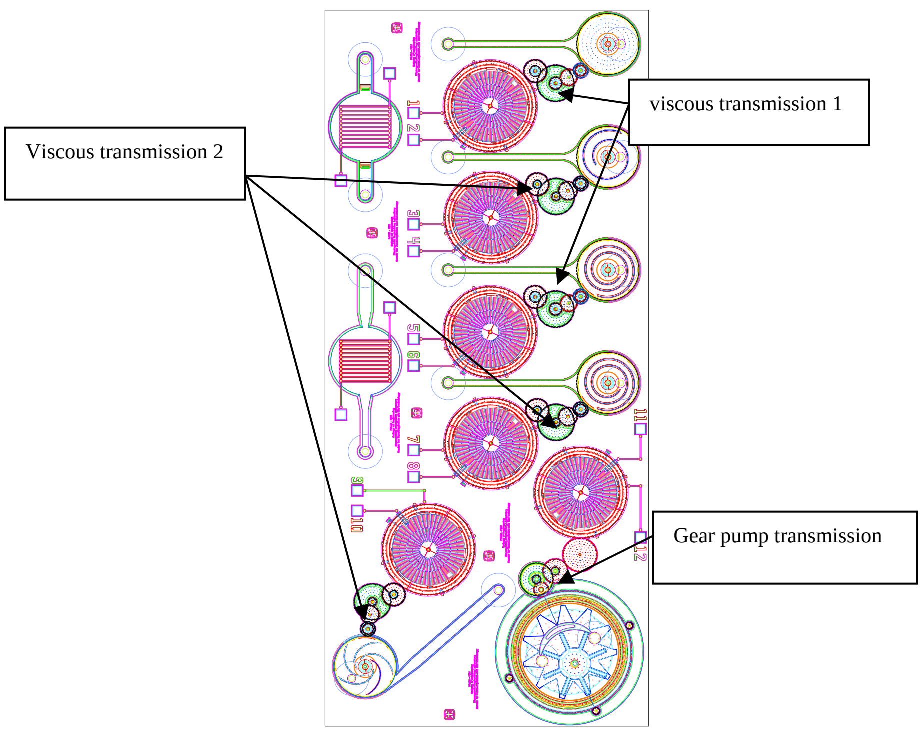


Figure 2. RS415 module 7 designs

On RS424 module 2, designed by Brian Sosnowchick, there are 4 new spiral viscous pumps, on new impeller pump and one new viscous plate pump driven by 1000:1, 2000:1, and 3000:1 transmissions (see Fig. 3).

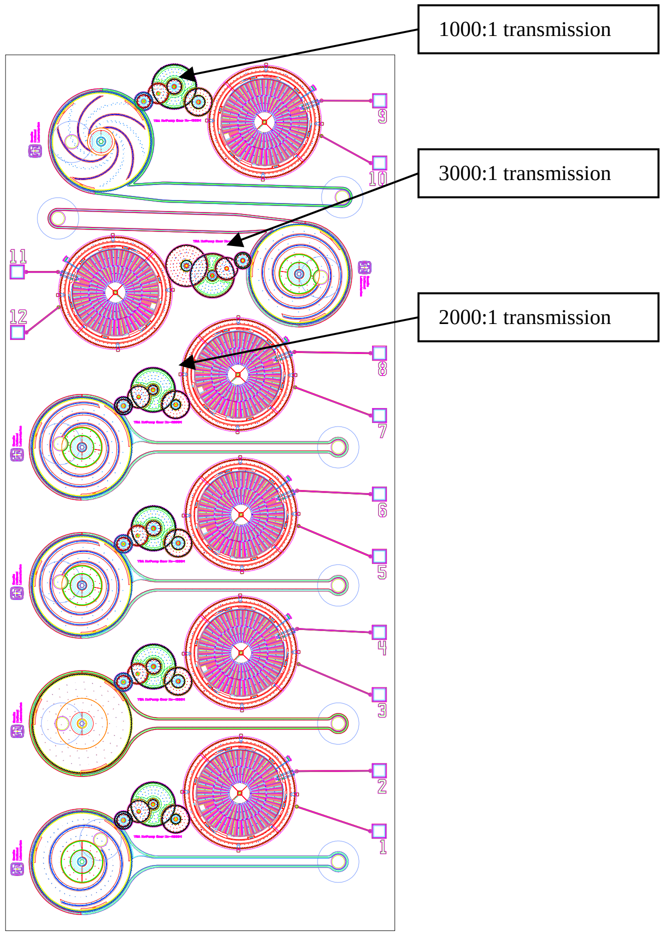


Figure 3. RS424 module 2 designs.

The gear ratio (e) defines the ratio of gear speeds at each end of the transmission. The torque ratio delivered is the inverse of this ratio, assuming 100% power transmission efficiency (friction ignored). Table 1 summarizes all the transmission designs for comparison. The pump gear is included in the transmission gear ratio calculation. The one non-TRA transmission (orthogonal comb drive) is included because it was the highest gear ratio transmission fabricated even thought it was unreliable and very little characterization was possible with this actuator/transmission combination.

| Design # | Description | $e = \frac{\#\, driving\ teeth}{\#\, driven\ teeth} = \frac{n_l\,(speed\ of\ last\ gear)}{n_f\,(speed\ of\ first\ gear)}$ | $\frac{1}{e} = \frac{torque\ at\ last\ gear}{torque\ at\ first\ gear}$ |
|---|---|---|---|
| 1 | RS275 crescent | 0.061 | 16.39 |
| 2 | RS275 simple viscous | 2.22 | 0.45 |
| 3 | RS275 complex viscous | 0.185 | 5.4 |
| 4 | RS275 orthogonal comb | 0.0166 | 60 |
| 5 | RS415 crescent gear | 0.061 | 16.39 |
| 6 | RS415 viscous #1 | 0.322 | 3.10 |
| 7 | RS415 viscous #2 | 0.161 | 6.21 |
| 8 | RS424 1000:1 | 0.24 | 4.17 |
| 9 | RS242 2000:1 | 0.12 | 8.33 |
| 10 | RS424 3000:1 | 0.08 | 12.50 |

Table 1.0  Gear and speed ratios for transmissions and torque ratio

## Pump Torque

The torque delivered by the TRA at a given voltage (Eqn. 3 and 4 above) multiplied by the amplification factor supplied by the transmission (last column of table 1) is the torque delivered to the pump gear. Fig. 4 shows plots of pump gear torque as a function of actuation voltage for each TRA/transmission combination fabricated on RS275 (1st generation), RS415 and RS424 (2nd generation).

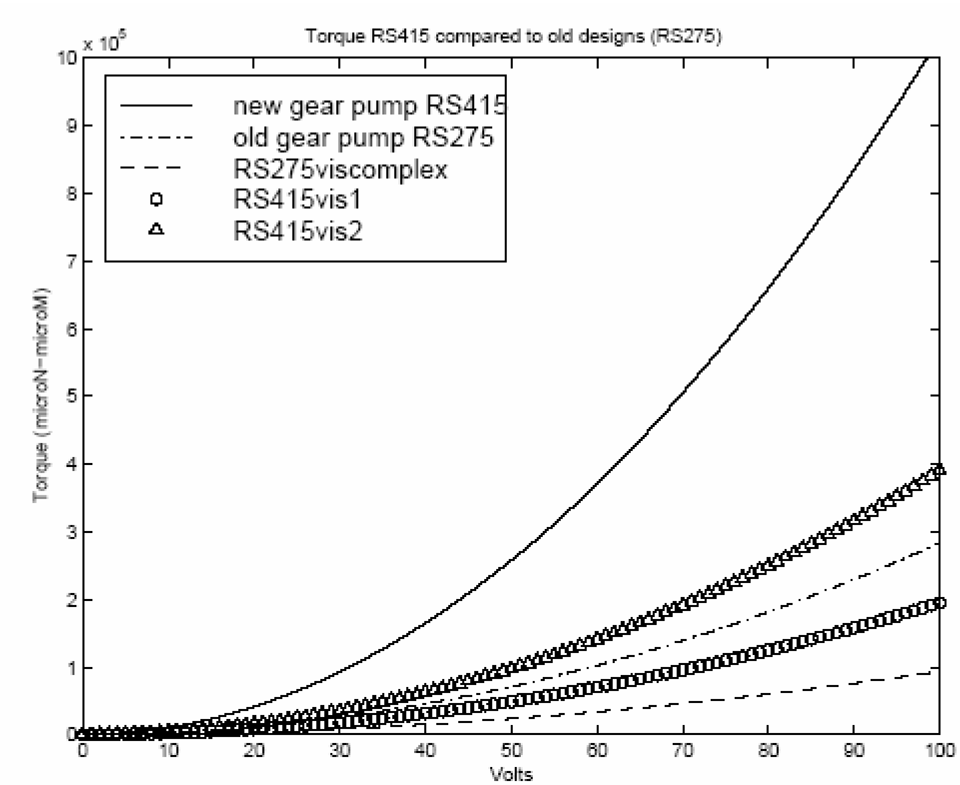


Figure 4a. Torque curves – Torque delivered to the pump for voltage input to TRA. Comparison of 1st generation design (RS275) with new designs on RS415. The simple transmission on the RS275 design produced very little torque and is not plotted. The new gear pump transmission and TRA delivers the most torque.

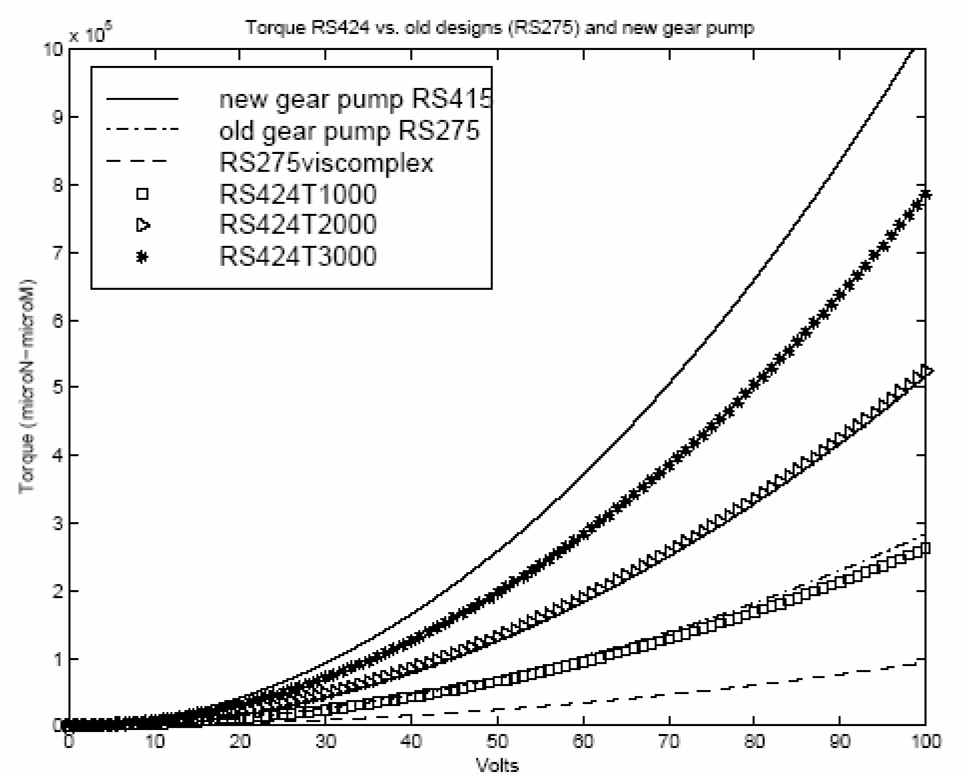


Figure 4b. Torque curves – Torque delivered to the pump for voltage input to TRA. Comparison of 1st generation designs (RS275), new gear design RS415 and new designs on RS424. The old gear pump (RS275) TRA/transmission delivers similar torque as the T1000 TRA/transmission design on RS424, but uses a lower power actuator with a higher gear ratio transmission.

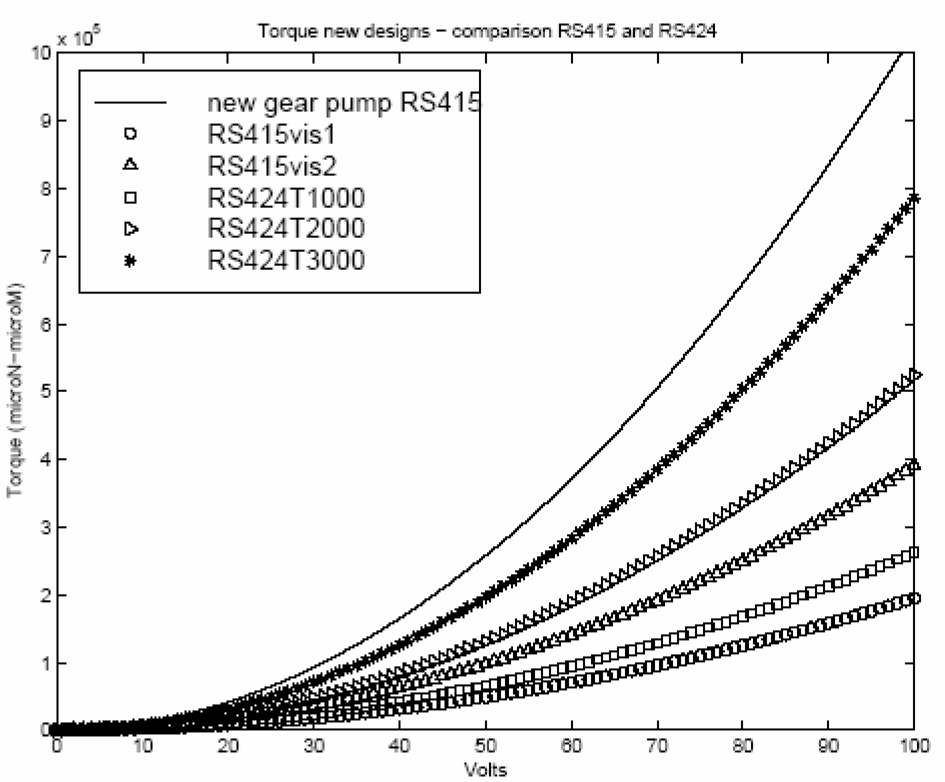


Figure 4c. Torque curves – Torque delivered to the pump for voltage input to TRA. This figure has the same data as Fig. 4a and 4b but with new designs only plotted. The highest torque was delivered to new gear pump on RS415 and the 2nd highest using the T3000 transmission and the redesigned TRA and RS424.

The equations for the torque curves (μN-μm) obtained by multiplying the appropriate equation (3) or (4) by the transmission torque ratio (table 1) are:

Equation (5)

(a) $T = 0.779 \times V^2$ for the simple gear train viscous pump and old TRA (RS275) – not plotted
(b) $T = 9.340 \times V^2$ for the complex gear train viscous pump and old TRA (RS275)
(c) $T = 28.35 \times V^2$ for the old crescent gear pump transmission with old TRA (RS275)
(d) $T = 19.50 \times V^2$ for the 1st transmission design for viscous pumps with new TRA (RS415)
(e) $T = 39.06 \times V^2$ for the 2nd transmission design for viscous pumps with new TRA (RS415)
(f) $T = 103.1 \times V^2$ for the new crescent gear pump transmission with new TRA (RS415)
(g) $T = 26.23 \times V^2$ for the new TRA and transmission (T1000 – 1000:1) (RS424)
(h) $T = 52.30 \times V^2$ for the new TRA and transmission (T2000 – 2000:1) (RS424)
(i) $T = 78.63 \times V^2$ for the new TRA and transmission (T3000 – 3000:1) (RS424)

## Pump Speed

The frequency of ratchet actuation divided by number of teeth gives the frequency of the TRA drive. Multiplying this frequency by the speed ratio defined by the transmission (3rd column in Table 1) gives the frequency of pump gear actuation. Fig. 5 shows plots of gear pump frequency as a function of actuation frequency for the same TRA/transmission combinations. The T1000 transmission refers to the 1000:1 reduction in frequency between the frequency of the signal applied to the TRA and the frequency of the last gear (in Hz); likewise for the T2000 and T3000 transmissions (all on RS424).

The equations used to generate the pump speed curves (Hz) in Fig. 5 as described in the preceding paragraph are:

Equation (6)
(a) $f_{pump} = 0.01350\ f_{drive}$ for the simple viscous pump transmission and old TRA on RS275 (not plotted)
(b) $f_{pump} = 0.00113\ f_{drive}$ for the complex viscous pump transmission and old TRA on RS275
(c) $f_{pump} = 0.00037\ f_{drive}$ for the gear pump transmission and old TRA on RS275
(d) $f_{pump} = 0.00025\ f_{drive}$ for gear pump transmission and new TRA on RS415
(e) $f_{pump} = 0.00134\ f_{drive}$ for the viscous pump transmission 1 and new TRA on RS415
(f) $f_{pump} = 0.00067\ f_{drive}$ for the viscous pump transmission 2 and new TRA on RS415
(g) $f_{pump} = 0.00100\ f_{drive}$ for the T1000 transmission and new TRA on RS424
(h) $f_{pump} = 0.00050\ f_{drive}$ for the T2000 transmission and new TRA on RS424
(i) $f_{pump} = 0.00033\ f_{drive}$ for the T3000 transmission and new TRA on RS424

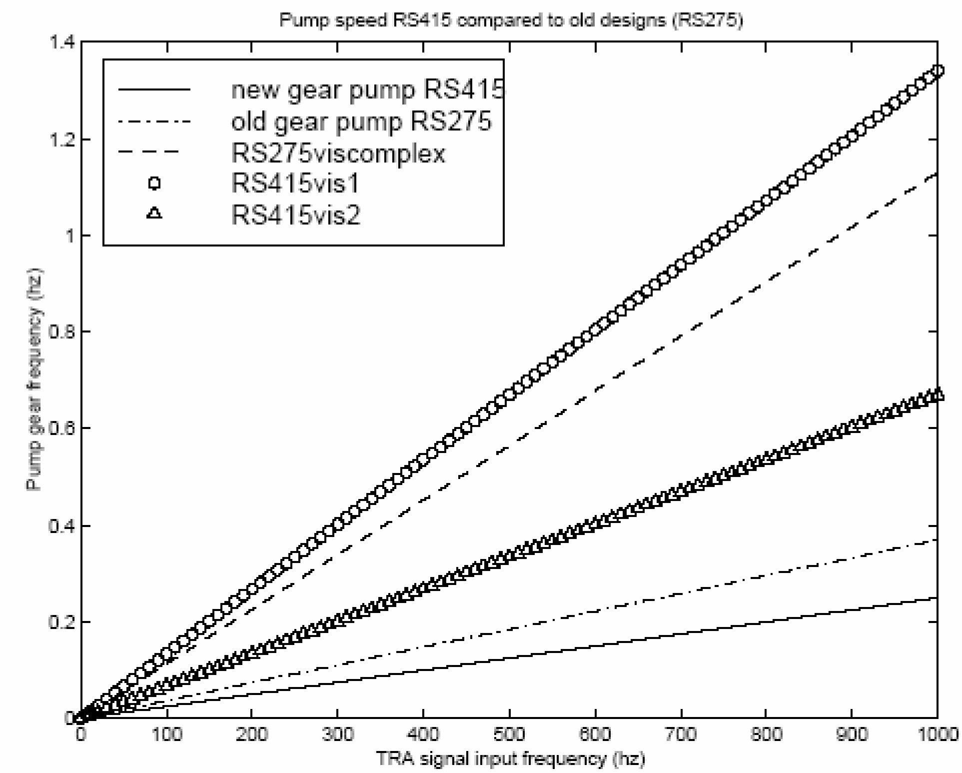


Figure 5a. Pump speed curves. Pump speed a function of input frequency for new RS415 designs compared to ol RS275 designs.

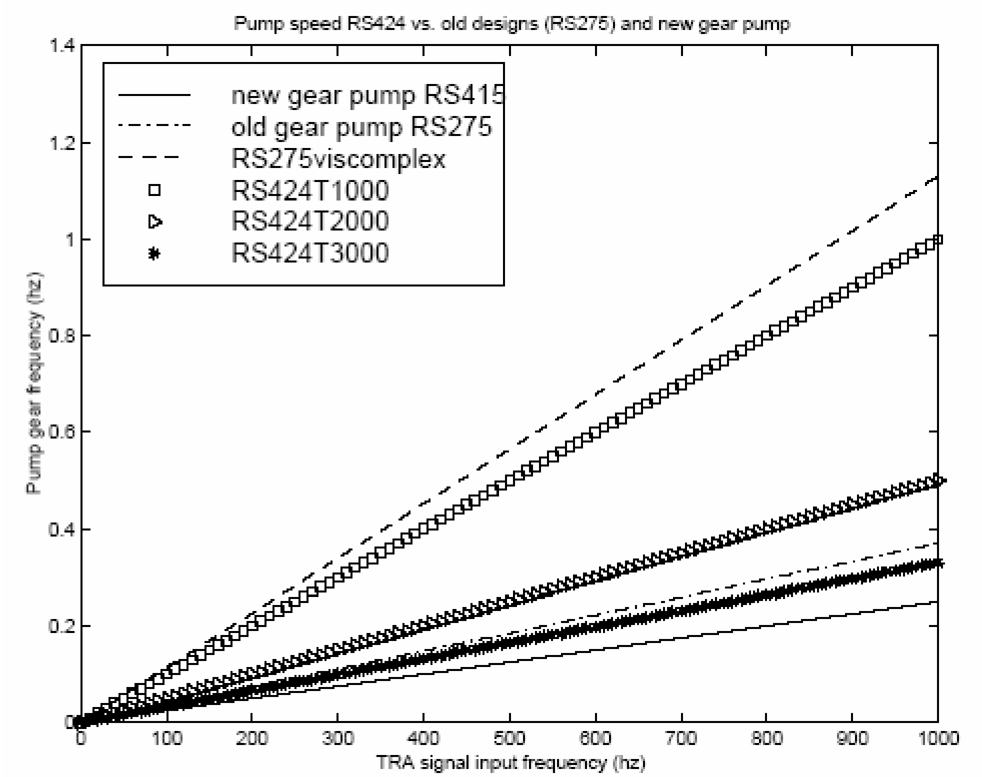


Figure 5b Pump speed curves. Comparison of new designs RS424 with old RS275 designs.

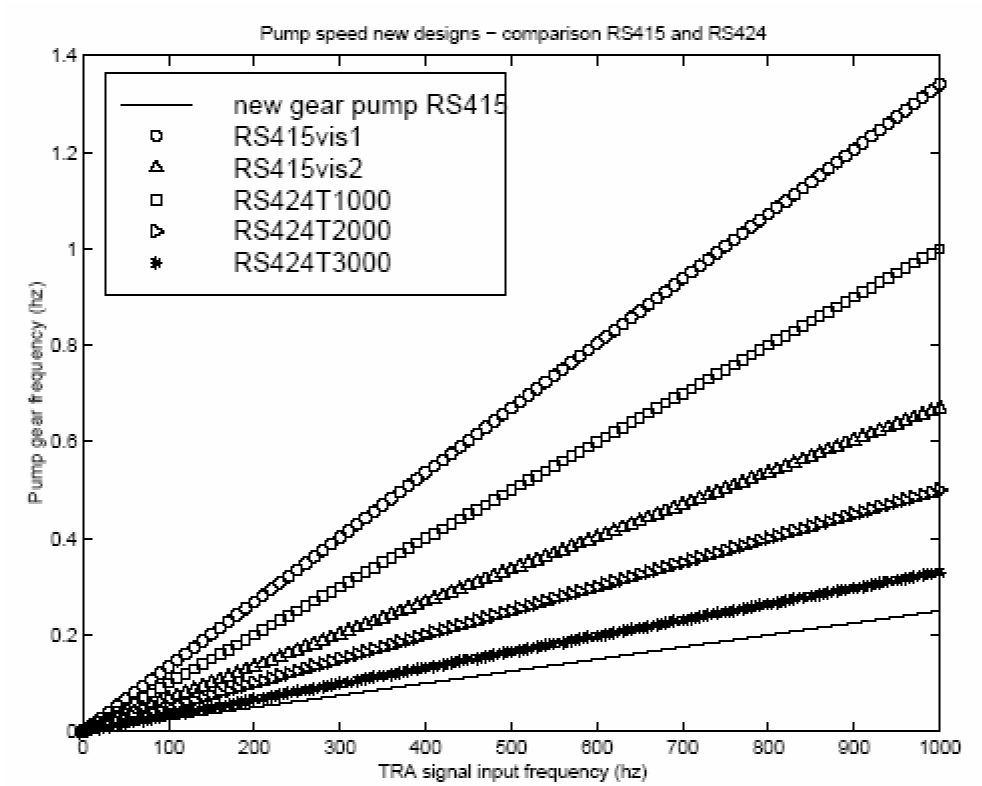


Figure 5c. Pump speed curves. Comparison of RS415 and RS424 new designs.

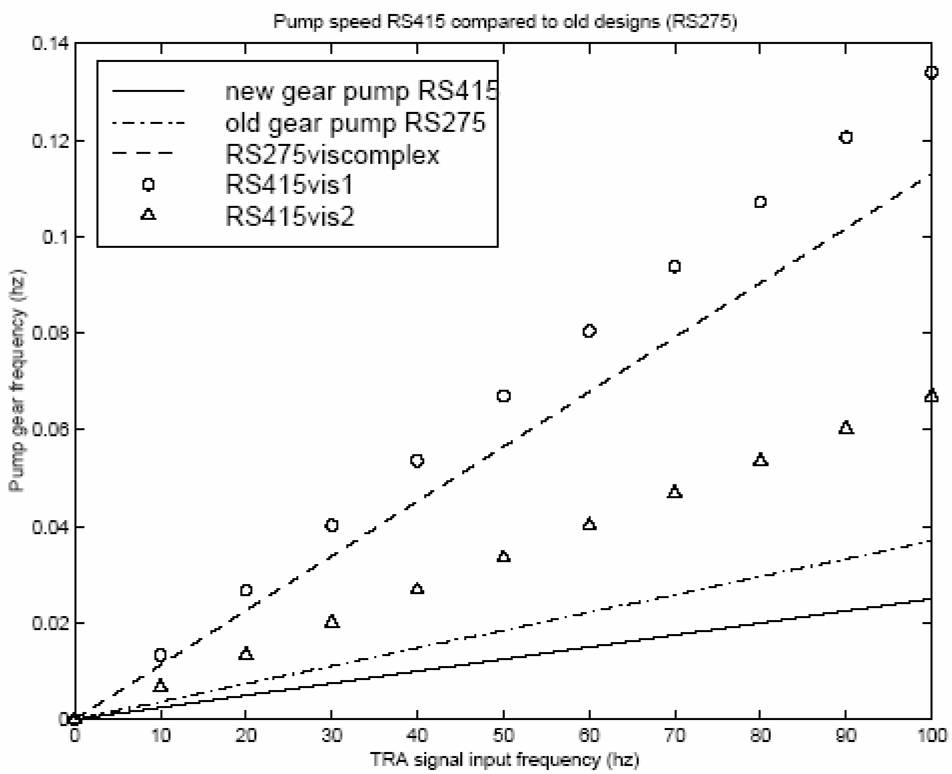


Figure 5d. Same data as Fig. 5a but zoomed in to 0 to 100 Hz input frequency range.

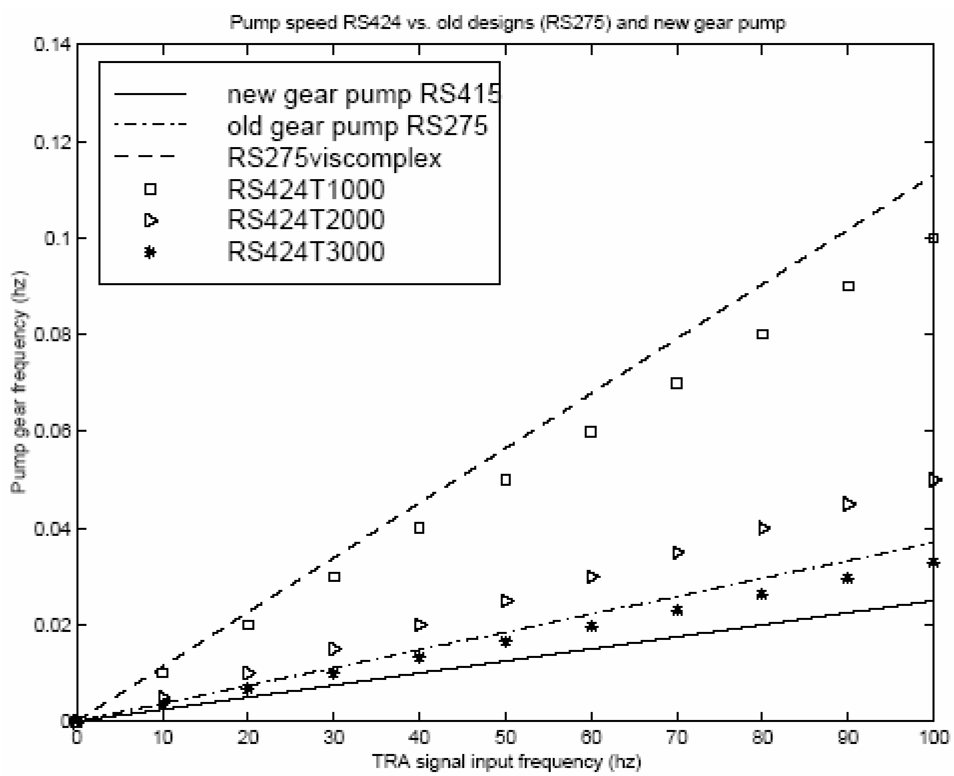


Figure 5e. Same data as Fig 5b but zoomed in to 0 to 100 Hz input frequency range.

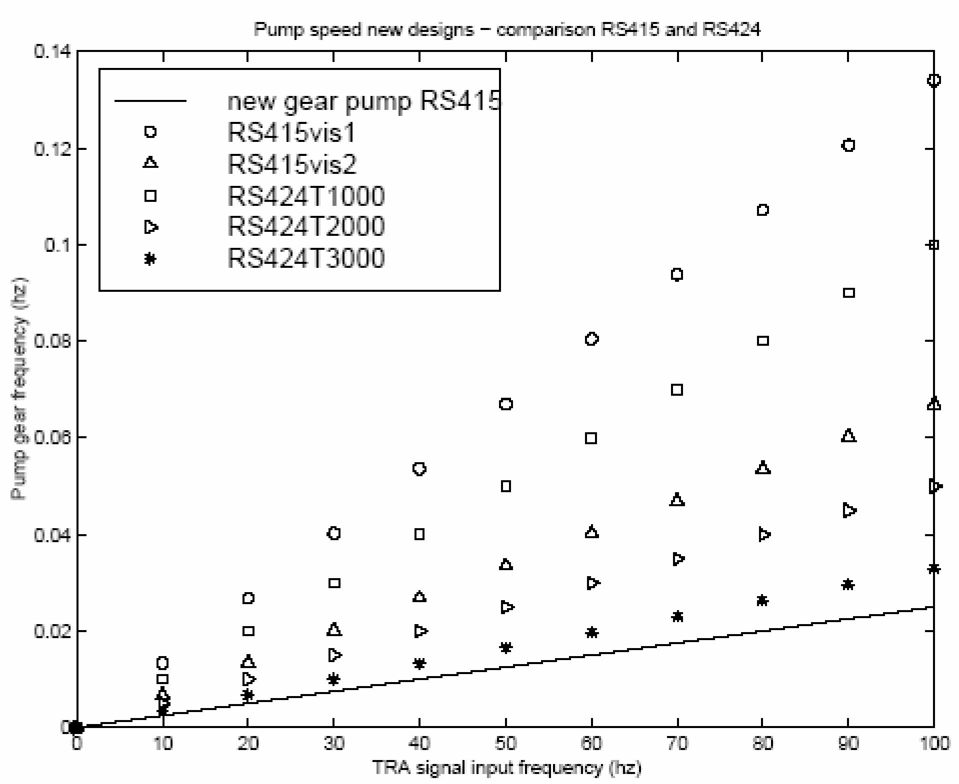


Figure 5f. Same data as Fig. 5c but zoomed in to 0 to 100 Hz range.

## TRA/Transmission/Pump testing

While we have not yet done a thorough dry actuation characterization, as was done for the 1st generation designs [6], preliminary dry testing indicates that the new TRA/transmission/pump designs (RS415 and RS424) performed better than the previous 1st generation designs (RS275). The first batch of the new designs generally appeared to start actuating at lower voltages and actuated to higher frequencies than the 1st generation designs. The SMM actuator/transmission/pump assemblies operated for a longer period of time before failure and between failures, allowing a pump curve to be generated, a process which requires continuous pump operation for an hour or more in order to allow a range of parameters (back pressure, applied voltage and frequency) to be varied while measuring flow rate by timing the motion of the meniscus in a connecting tube downstream of the pump. The first batch of pumps exhibited fewer failure modes then the earlier pump designs (RS275) – the trace shorting problem, rocking problem and ratchet tooth skipping problems exhibited in the 1st generation designs [6,7] were not observed. The primary failure mode was the stuck-open and/or stuck-closed mode. Further testing is required in order to determine the relative frequency of occurrence of these two failure modes. A single poke with a probe tip was generally sufficient to free the stuck TRA comb drive and cause actuation to resume.

The highest torque actuator (gear pump on RS415 – see Fig. 5 above) was the most reliable in terms of likelihood of starting the first time without probing and longest continuous actuation without sticking. It also began actuating at a relatively low voltage of 10-20 V and once even began actuating without any voltage applied at all when Jason Hendrix brought either his hand or probe tips near the actuator. There are several possible explanations for this phenomena including; static charge build-up and dissipation, and noise from instruments near the MEMS chip that is picked up by structures on the MEMS chip that act as micro-antennas.

While the initial assessment of the 2nd generation designs was positive, the 2nd group of pumps tested dry were more unreliable, leading us to consider a DOE (Design of Experiments) to isolate failure modes for the 2nd generation designs. The DOE is outside the scope of this report.

## Gear pump testing

The 2$^{nd}$ generation gear pump/TRA/transmission or RS415 (module 7) successfully pumped water both at FSU and here at Sandia (2 separate pumps – one tested at FSU and one at Sandia). The testing procedure was as follows:

(1) Dry actuate the gear pump.

Determine that the pump could be reliably actuated dry by applying low voltage (15-30 V) square wave signal at a low frequency (1-3 Hz) to the TRA. At this low frequency any problems with the actuator or transmission motion can be observed. Ramp up the actuation frequency to around 100 Hz to verify smooth higher frequency operation of the entire SMM actuator/transmission/pump system.

(2) Plumb the MEMS module.

Attach 300 μm outer diameter stainless steel capillary tubes to the back of the die at the pump inlet and outlet by inserting them into the Bosch-etched counterbore holes and gluing them in place using superglue and/or epoxy. The gear pump inlet and outlet are on the bottom of the gear pump housing beneath the moving gear teeth and are connected to from the back side through Bosch etched vias through the wafer. Figure 6 is an image of the gear pump from the 1$^{st}$ generation design with the housing cover removed. The Bosch connecting inlet and outlet holes are clearly visible. The 1$^{st}$ and 2$^{nd}$ generation gear pumps and transmissions are identical, however the new TRA actuator allows significantly higher torque to be delivered to the pump gears (Fig. 4 curves).

(3) Attach tubing and set up pressure head and flow rate control.

See Fig. 7 (test setup)

(4) Prime the pump.

Fill the inlet tube to the stainless steel capillary using hydrostatic pressure (head). Actuate the device at a low frequency (e.g. 38 V square or sine wave at 3 Hz). Switch the 3-way valve upstream of the device from hydrostatic pressure to the syringe pump. Set syringe pump flow rate to 200 μl/hr and pump liquid through the MEMS pump until the meniscus is clearly visible in the downstream tube and all air bubbles have been flushed from the system.

(5) Set pressure head, apply signal of interest, and measure flow rate during pump actuation by timing the motion of the meniscus in the known cross-sectional area outlet tube.

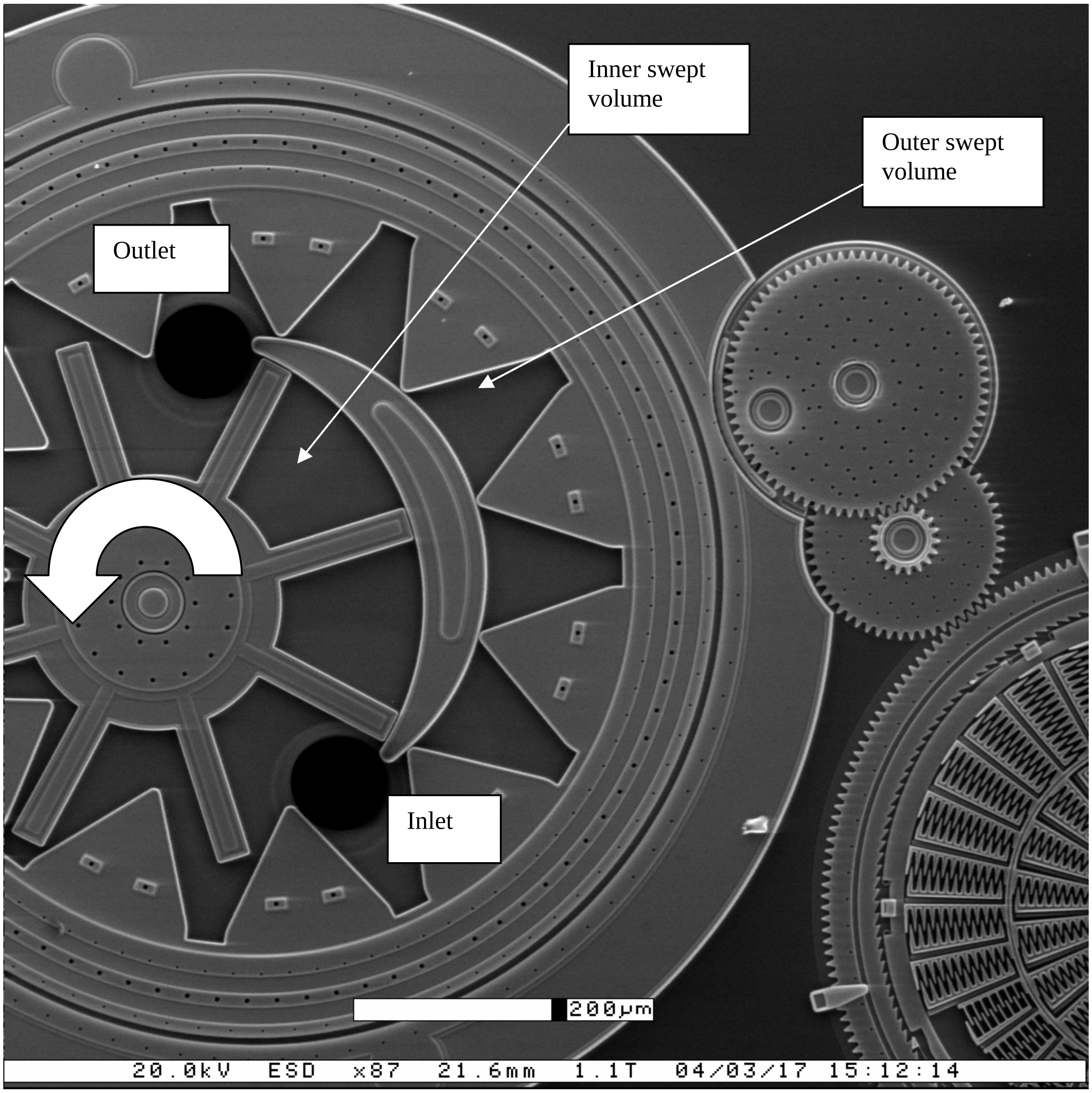


Figure 6. SEM showing gear pump with cover removed.

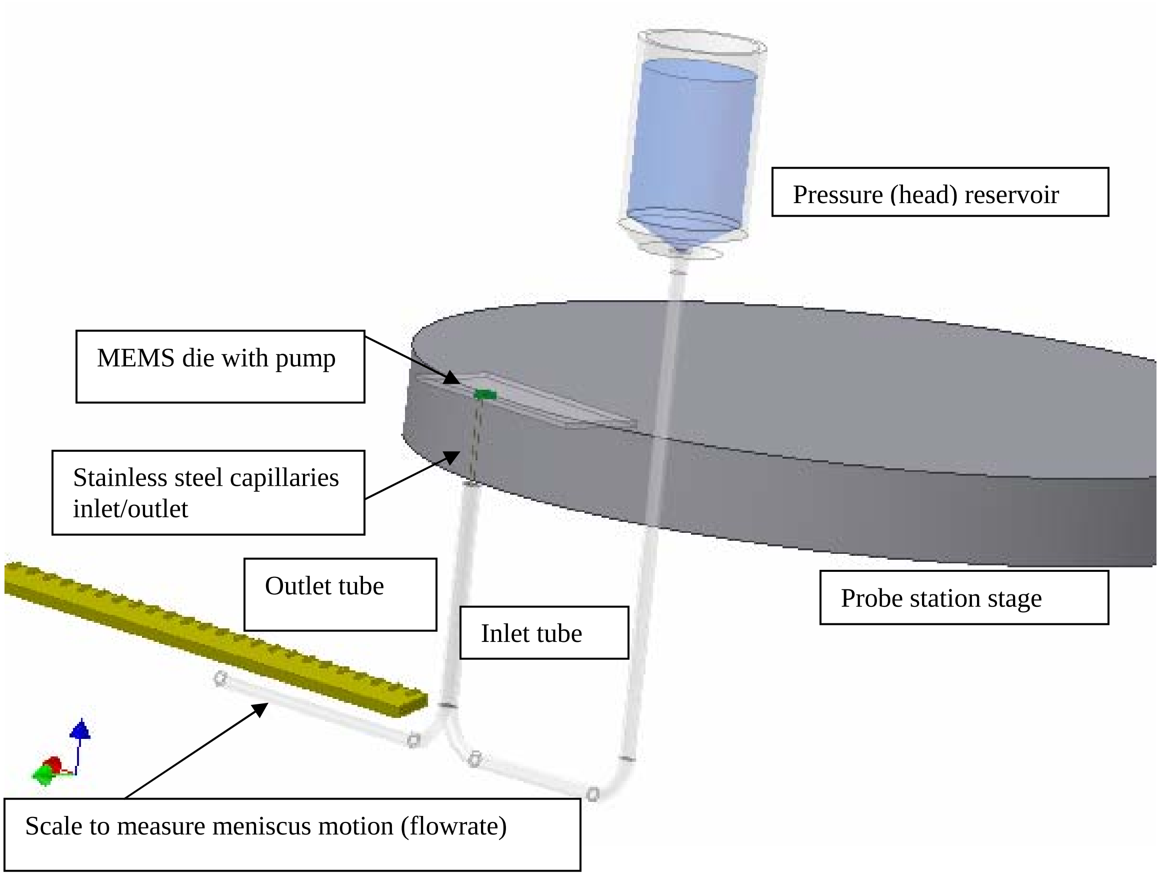


Figure 7. Test setup. Microscope above MEMS die to observe pump operation not shown. In our setup a 3-way valve and syringe pump allowing either upstream pressure or flow control is used – also not shown.

## Test Results – gear pump testing

The gear pump was tested both at FSU and Sandia (two different die). In both locations the test was conducted at zero back pressure. At Sandia the effect of pump speed was investigated by varying the frequency of the drive signal and the effect of back pressure was investigated by varying the back pressure on the downstream end of the pump. The effect of the actuation frequency is shown in Fig. 8 below. The test data from FSU is also included and consists of a single data point: pump flow rate measured for zero back pressure, square wave actuation at 50 V and 8 Hz. For these conditions a flow rate of 0.54 nl/s was generated at FSU and a similar flow rate at Sandia. The power supply used at FSU created a noisy signal which made it difficult to test at other conditions. The pump operated continuously for approximately 1.5 hours during this test despite the poor quality signal from the power supply.

The tests at Sandia utilized the high frequency power supply designed by Ken Pohl (dept. 1769). The voltage of 38 V was chosen after slowly increasing voltage and monitoring ratchet actuation during pumping. At approximately 30 V smooth actuation commenced. Therefore a voltage of 38 V was chosen to provide some cushion above the first point of smooth actuation. Voltages above that required for smooth ratchet actuation will not result in a higher flow rate as the pump speed is set by the actuation frequency. If as actuation frequency is increased the ratchet actuation begins to be marginal at a given voltage (not consistently engaging the next ratchet tooth) increasing the voltage provides a means of applying more torque and re-establishing smooth operation. In the data shown this phenomena was not observed, ratchet actuation was similar for all frequencies and did not degrade at the higher frequencies.

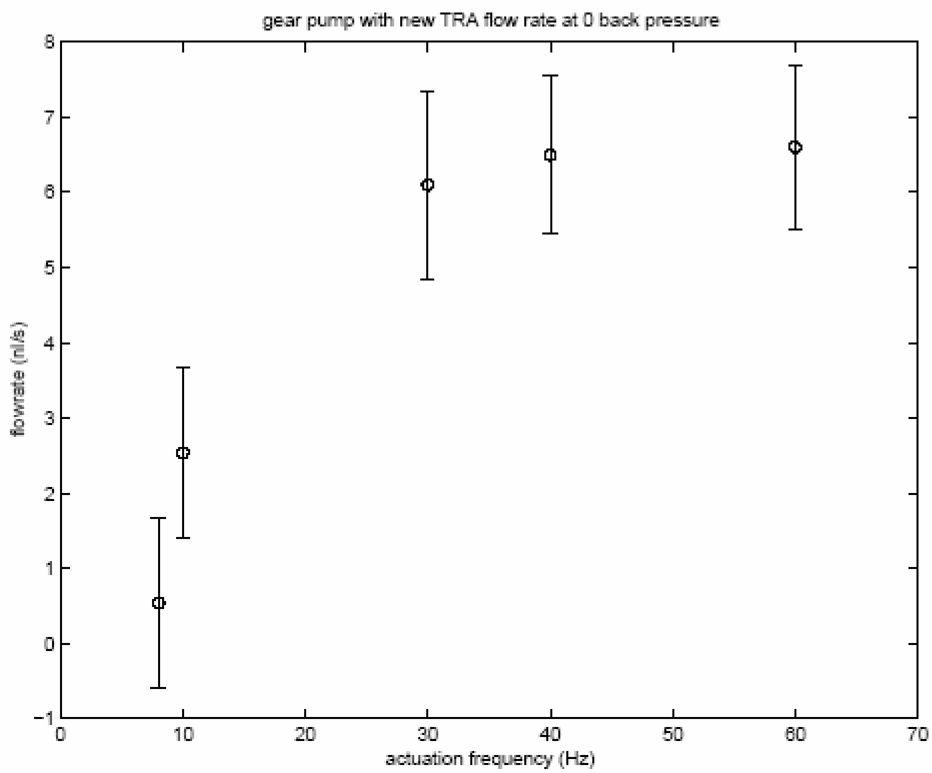


Figure 8. Flowrate at zero back pressure as a function of actuation frequency – crescent gear pump with new TRA – 38 V square wave actuation signal for all but 8 Hz data which was at 50 V.

The pump curve (Fig. 8) shows that a maximum flow rate of approximately 5 nl/s is generated at the frequency at which the curve levels off (40-60 Hz actuation signal frequency). The pump frequency is approximately 0.01 Hz (0.6 RPM) at this actuation frequency (Fig. 5) and the torque delivered is ~18 μN-μm at 38 V (Fig. 4) for these maximum flow conditions.

Fig. 9 shows the effect of back-pressure on flowrate at a single operating signal (30 V at 10 Hz square wave). The back pressure was negative for most of the data because the meniscus was below the pump module through most of this test.  Unfortunately the pump failed as we went to higher back pressures.  It is unclear at this time whether this was just a coincidence – the pump had been operating for at least an hour – or whether the pump is unable to operate at a significant back pressure (several psi).

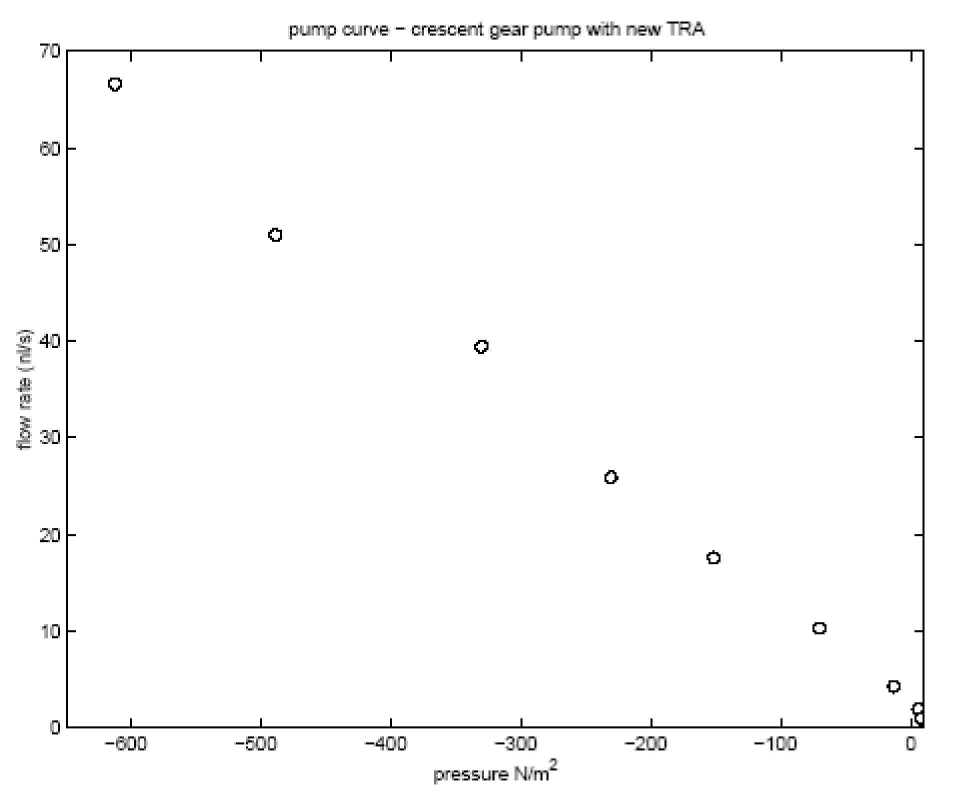


Figure 9.  Pump Curve.  Flow rate for different back pressures at 10 Hz 30 V square wave actuation signal.

The negative pressure levels do not lead to significant flow through the MEMS pump.  At the largest negative back pressure (-600 N/m$^2$) the flow rate as calculated for Poiseuille flow through the pump and tubing would only be about 10 nl/s, so the bulk of the flow rate generated is due to pump actuation not the negative pressure gradient across the pump.

## Conclusions and Further Work

This LDRD not only demonstrated conceptually and qualitatively that this class of micropumps can effectively move fluid, but quantitatively measured how much fluid was moved at what conditions. This is a significant breakthrough for microfluidic systems, which as is the case for MEMS in general, often are hard to characterize beyond the initial – 'yeah it works' – stage. Now we need to develop more reliable pump/transmission/TRA actuator and characterize the device across a wide range of operating conditions of specific interest for a variety of applications.

The work on this LDRD was a good start on characterizing this class of surface micromachined pumps, however a significant amount of work remains before the next generation pumps can be designed and microfluidic chips utilizing the pumps for specific applications can be developed. In other words, work is needed to turn this promising concept into a work-horse pump that can be inserted into a variety of systems to provide precise fluid delivery. Specifically the following tasks should be undertaken in order to fully characterize the existing pumps:

(1) Crescent gear pump. Develop a full family of pump curved similar to Fig. 8 but at different back pressures; including the negative back pressures of Fig. 9 and positive back pressures. For instance each point on Fig 9 would have a curve going through it similar in shape to the curve shown in Fig. 8. Try to develop pump curves for different viscosity liquids.
(2) Highest torque spiral pump (3000:1 transmission on RS424). This pump/transmission/TRA should have adequate torque to produce a pump curve. Attempt to characterize this device in the same manner that the crescent gear pump is characterized.
(3) Dry testing of both crescent gear pump, and highest torque spiral pump (and perhaps other pumps) to isolate causes of sticking (open and/or closed). Investigate two hypotheses regarding sticking: (a) sticking caused by electrostatic charge buildup, (b) sticking caused adhesives fumes depositing on comb structures during the capillary gluing process. Determine an optimum signal to reduce the incidence of sticking as was done for the previous pump designs [6]. Determine an optimum release time and drying process to reduce sticking.
(4) Develop a more accurate and faster method of measuring flow rate at the low flow rates of interest. Measuring the movement of the meniscus takes significant time and effort and has a large error associated with it.

Item (3) in this list probably needs to be accomplished first in order get more consistently reliable pump operation as would be required for items (1) and (2). Item (4) would significantly reduce the time required to accomplish items (1) and (2) and therefore would be worth accomplishing before (1) and (2). By accomplishing the items in this list we can make a much more informed redesign of these pumps for specific microfludic applications, as well as get a very clear understanding of how these pumps operate in a wide range of conditions.

## References:


1. Nguyen N-T, Huang X, Chuan T K, 'MEMS-Micropumps: A Review', Transactions of the ASME Journal of Fluids Engineering, Vol. 124, June 2002.
2. Paul P, Arnold D W, Rakestraw D J, 'Electrokinetic Generation of High Pressures Using Porous Microstructures', Proceedings of μTAS 98 workshop, October 1998.
3. SAND2002-3988, 'New Architectures for Micro-Total-Analytical Systems', Galambos P C, Pontau A, Okandan M, Kirby B J, Shepodd T J, James C D, and Pohl K, December 2002.
4. Kilani M, Haik Y, Chen C-J, Galambos P, "A Surface Micromachined Spiral Channel Viscous Pump", Proceedings of the ASME International Conference and Exposition (WAM), New Orleans LA (Nov 2002), IMECE2002-33667.
5. Jeff Lanz – revised TRA – personal communication and powerpoint presentation.
6. Sosnowchick B D, Galambos P, Sharp K V, Jenkins M W, Horn M W, Hendrix J, "Dry Actuation Testing of Viscous Drag Micropumping Systems for the Determination of Optimal Drive Waveforms", Proceedings of SPIE/Photonics West – Microfluidics and BioMEMS, (January 2004).
7. Galambos P, Sosnowchick B, Hendrix J, and Zwolinski A, SAND2003-4674 'Development of Highly Integrated Magnetically and Electrostatically Actuated Micropumps',

## Distribution:

| | | |
|---|---|---|
| 2 | MS 1080 | Paul C. Galambos, 1769 |
| 1 | MS 1080 | David R. Sandison, 1769 |
| 1 | MS 1080 | Jamie Reif, 1769 |
| 1 | MS 1080 | Conrad James, 1769 |
| 1 | MS 1080 | Mark Jenkins, 1769 |
| 1 | MS 1080 | Jeff Lantz, 1769 |
| 1 | MS 1080 | Jim Allen, 1769 |
| 1 | MS 1080 | Murat Okandan, 1749 |
| | | |
| 1 | MS 1077 | Thomas Zipperian, 1740 |
| 1 | MS 1079 | Marion Scott, 1700 |
| | | |
| 1 | MS 9018 | Central Technical Files, 8945-1 |
| 2 | MS 0899 | Technical Library, 9616 |
| 1 | MS 0323 | D. Chavez, LDRD Office, 1011 |